UCRL- 93552
PREPRINT

PATH INTEGRAL COMPUTATION OF THE LOW TEMPERATURE PROPERTIES OF LIQUID ^{4}He

D. M. Ceperley and E. L. Pollock
Lawrence Livermore National Laboratory
University of California
Livermore, CA 94550

This paper was prepared for submittal to
Physical Review Letters

October 1985

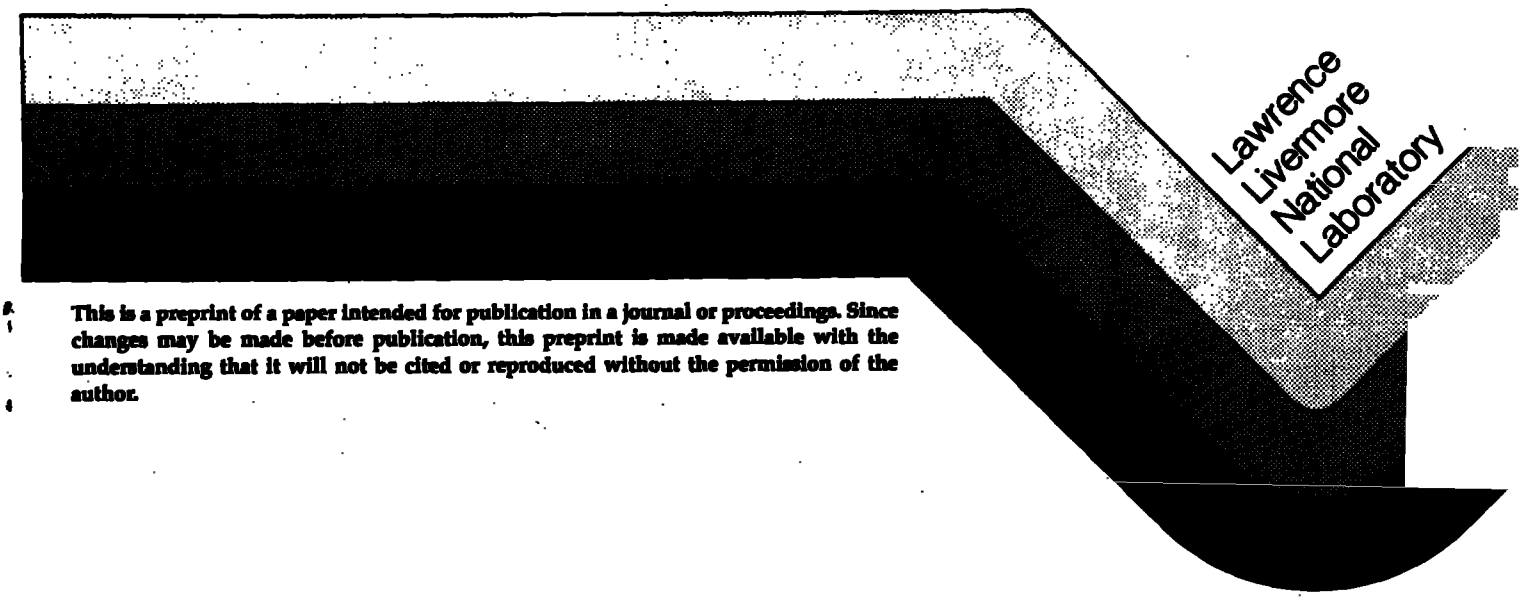

PATH INTEGRAL COMPUTATION OF THE LOW TEMPERATURE PROPERTIES OF LIQUID ^{4}He

D. M. Ceperley and E. L. Pollock
Lawrence Livermore National Laboratory
University of California
Livermore, CA 94550

Discretized path integral computations of the energy, structure factor, radial distribution function and momentum distribution of ^{4}He in good accord with experiment are presented for temperatures down to 1°K at saturated vapor pressure.

The unusual properties of liquid ^{4}He at low temperature were attributed to Bose-Einstein condensation by F. London in 1938.[1] The strength of the pair interaction between helium atoms however, has so far prevented a first principles study of this transition in ^{4}He. In this letter we present a Monte Carlo discretized path integral computation of the density matrix for liquid ^{4}He for temperatures spanning this transition which reproduces many of the experimental results and is in principle capable of arbitrary accuracy. We have assumed that the atoms interact via the Aziz pair Potential.[2]

The calculations for the many body density matrix,[3]

$$\rho(R,R';\beta) = \langle R|e^{-\beta H}|R'\rangle \tag{1}$$

from which all equilibrium properties can be obtained, are based on the identity

$$\rho(R,R';\beta) = \int \cdots \int \rho(R,R_1;\tau)\rho(R_1,R_2;\tau) \cdots \rho(R_{M-1},R';\tau)\, dR_1 \cdots dR_{M-1} \tag{2}$$

where $\tau = \beta/M$, $M>1$, and the R variables denote points in the 3N dimensional coordinate space. If an accurate many body density matrix is known at some high temperature corresponding to τ then equation 2 allows its calculation at a lower temperature $T = 1/Mk\tau$. The density matrix for Bose systems is obtained by summing over all permutations of particle labels.[3]

$$\rho_B(R,R';\beta) = \frac{1}{N!}\sum_P \rho(R,PR';\beta) \tag{3}$$

Both the integral over paths and the sum over permutations are performed by a generalization of the Metropolis Monte Carlo method. A discussion of how this is implemented for distinguishable particles is given in Ref. 4. In extending this work to bosons several new techniques were required which will be described in detail elsewhere but before presenting our results we briefly mention two of the most important.

First (as in Ref. 4) the many body density matrix at high temperature in Eq. (2) is taken as a product of one and two body density matrices which is exact in the high temperature limit. Here we have used the full two body density matrix rather than the "end-point" approximation of earlier work. This is more accurate and allows larger values of τ (smaller M) to be used in Eq. (2). The high temperature density matrix used was typically for a temperature of 40 °K and thus paths of about 20 steps were needed for computations near T_λ. Had we been interested in only the structural properties rather than, for example the kinetic energy, steps corresponding to 20 °K or less would have sufficed. We have checked the adequacy of the step size by rerunning selected points using 80 °K steps. A thorough convergence study of the earlier method was done in.[4]

Secondly a new method was used to construct trial paths for the multi-particle moves necessary in sampling the permutations of Eq. (3). The particular particles (here as many as 4) for which permutation changes are attempted at one Monte Carlo move are initially selected based on the free particle density matrix. New trial paths are then generated by a "bisection method" which first generates new midpoints for paths and then new midpoints for the remaining halves and so on with the possibility of rejecting the new paths at any stage in the construction.

For permutations this is more efficient than the previous method of sequentially generating new paths step by step since now improbable paths may be rejected at an early stage in their construction thus allowing many more trial moves for a given amount of computer time. The rejection step ensures that the accepted permutations and paths reflect the correct density matrix and not our initial guesses. Extensive tests of the convergence of the distribution of permutations were carried out.

Table I lists some of the temperatures and densities at saturated vapor pressure (SVP) along with the potential and kinetic energy and some structural properties where computations were done. The computed energy and specific heat as a function of temperature at SVP near T_λ are compared with experiment in fig. 1. The simulations are for a periodic system of 64 atoms and each run takes about one hour on the CRAY-1. The finite number of particles used in these simulations apparently depresses the computed energy in the temperature region $2.1°K<T<3°K$.

The effect of Bose statistics on the radial distribution function, g(r), is small as shown at T=2.0 °K SVP in fig. 2a where the neutron scattering results[8] are compared with the present simulation. The dashed line shown at the first peak and first minimum is for distinguishable particles (only the identity permutation is allowed in Eq. (3)) and shows the slightly increased spatial ordering attributed, via the uncertainty principle, to the decreased ordering in momentum space when the condensate is suppressed. Similar good agreement is obtained between the computed radial distribution and structure functions and the available neutron and X-ray[9] scattering data at other temperatures and pressures in the liquid phase.

The single particle momentum distribution, n(k), is the Fourier transform of the single particle off-diagonal density matrix, n(r)[10]

$$n(r) = \frac{\int \rho_B(r_1, r_2 \ldots r_n, r_1 + r, r_2 \ldots r_n; \beta) dr_1 \ldots dr_n}{\int \rho_B(r_1, r_2 \ldots r_n, r_1, r_2 \ldots r_n; \beta)\, dr_1 \ldots dr_n} \qquad (4)$$

which in terms of path integrals corresponds to one open path beginning at r_1 and ending at $r_1 + r$. (Here the r_i are the coordinates of atom i.) At temperatures well above T_λ where only the identity permutation is important, this open path involves only one particle and is restricted to a distance on the order of the thermal wavelength, $\hbar / \sqrt{2mkT}$. This is primarily due to the free particle part of the density matrix somewhat modified by many body effects. Below T_λ this open path may involve a long cyclic permutation of many particles and the end-to-end distance will become macroscopic. The n(r) in fig. 2b shows this change in character on going through the transition.[11] The initial curvature is proportional to the kinetic energy and the value at large r is the fraction of particles in the zero momentum state, the condensate. Figure 3a shows this condensate fraction as a function of temperature. The condensate fractions plotted there are obtained by assuming n(r) to be constant beyond 5Å and averaging the values between 5Å and 7Å to obtain $n_o(T)$. Near T_λ n(r) reaches its asymptotic value slowly and this procedure, because of the relatively small system simulated and periodic boundary effects, is not reliable. For example we find an n_o (T) value of 1.4% at 2.5 °K significantly above the experimental transition temperature. Larger systems must be considered to determine the condensate fraction near T_λ. The momentum distribution of the non-condensed particles, fig. 3b, is both non-Gaussian and has a temperature dependent shape. The present simulations are too noisy to adequately test the predicted low momentum singularities in this distribution.[13]

In the past estimates of the condensate fraction have been made[14] based on the hypothesis of Hyland, Rowlands, and Cummings[15] that the pair correlation function at large r has a constant shape below T_λ and is multiplied by $(1-n_0(T))^2$, (intuitively speaking the probability that neither atom in the pair is in the condensate and thus spatially uniform). We can only test this at moderate values of r but an estimate of $n_0(T)$ based on the second maximum, h_3, listed in table 1 does not conflict with our results. Estimates based on the first minimum, h_2, at smaller r seem definitely too small. Another intuitive estimate of $n_0(T)$ assumes the contribution of non-condensed atoms to the kinetic energy to be unchanged below T_λ where the condensate makes no contribution and thus the kinetic energy is proportional to $1-n_0(T)$. Fig. 3b suggests that this assumption is only approximate, nevertheless this estimate, using table I, also accords with our results due to the still sizeable error bars in the $n_0(T)$ estimates.

Efforts are underway to extend these simulations to larger systems and to determine other properties of ^{4}He.

ACKNOWLEDGEMENTS

Work performed under the auspices of the U.S. Department of Energy by the Lawrence Livermore National Laboratory under contract number W-7405-ENG-48.

0331M/0522M

REFERENCES

1. F. London, Nature 141, 643 (1938).
2. R. A. Aziz, V. P. S. Nain, J. S. Carley, W. L. Taylor and G. T. McConville, J. Chem. Phys. 70, 4330 (1979).
3. R. P. Feynman, "Statistical Mechanics", Benjamin, Reading Mass. (1972).
4. E. L. Pollock and D. M. Ceperley, Phys. Rev. B30, 2555 (1984).
5. R. K. Crawford in "Rare Gas Solids" Vol I, 663, edited by M. L. Klein and J. A. Venables, academic (1976).
6. J. Wilks, "Properties of Liquid and Solid Helium", Oxford, Clarendon (1967).
7. M. H. Kalos, M. A. Lee, P. A. Whitlock and G. V. Chester, Phys. Rev. B24, 115 (1981).
8. E. C. Svenson, P. Martel, V. F. Sears and A. D. Woods, Can. J. of Phys. 54, 2178 (1976).
9. H. N. Robkoff and R. B. Hallock, Phys. Rev. B24, 159 (1981).
10. O. Penrose and L. Onsager, Phys. Rev. 104, 576 (1956).
11. It is interesting to note that a formal correspondence between Bose-Einstein condensation and polymerization was noted over 35 years ago. W. H. Stockmayer and B. H. Zimm, Ann. Rev. of Phys. Chem. 35, 1 (1984) and references.
12. P. A. Whitlock, private communication of work in progress. For valves of r less than the de Broglie thermal wavelength the n(r) from the finite temperature simulations is of comparable accuracy with the ground state result. At larger r it proved necessary to actually simulate a system with one open path, as described in the text, and as seen in fig. 2b the scatter in the finite temperature results is greater there.
13. A. Griffin, Phys. Rev. B30, 5057 (1984).
14. V. F. Sears and E. C. Svensson, Int. J. of Quantum Chem. 14, 715 (1980).
15. G. J. Hyland, G. Rowlands, and F. W. Cummings, Phys. Lett. 31A, 465 (1970).

TABLE I

T(°K)	$\rho(\text{Å}^{-3})$	<U>/N (°K)	<K>/N (°K)	r_1(Å)	r_2(Å)	r_3(Å)	h_1	h_2	h_3
4.0	.01932	-18.91	15.65	2.973	4.583	6.271	.356	-.113	.040
3.333	.02072	-20.38	16.00	2.962	4.552	6.240	.369	-.126	.050
2.857	.02142	-21.14	15.99	2.950	4.537	6.234	.381	-.134	.055
2.50	.02179	-21.52	15.90	2.948	4.533	6.220	.383	-.136	.059
2.353	.02191	-21.60	15.75	2.945	4.526	6.205	.382	-.136	.060
2.222	.02197	-21.70	15.89	2.945	4.526	6.205	.382	-.139	.061
2.105	.02194	-21.57	15.10	2.940	4.522	6.205	.374	-.131	.055
2.0	.02191	-21.57	15.05	2.942	4.525	6.211	.377	-.132	.056
1.818	.02186	-21.44	14.71	2.939	4.526	6.209	.369	-.127	.053
1.600	.02183	-21.39	14.40	2.938	4.520	6.213	.368	-.124	.051
1.379	.02182	-21.35	14.23	2.937	4.515	6.206	.366	-.123	.050
1.1765	.02182	-21.35	14.17	2.938	4.520	6.212	.366	-.123	.050
2.0	.02191	-21.75	16.24	2.950	4.535	6.205	.385	-.140	.064

Computed potential and kinetic energies for various temperatures at SVP. The statistical uncertainty in the potential energy is about .04 °K and .08 °K in the kinetic energy. The densities used are based on ref. 5. The last six columns give the first three zeros and extremal values of the pair correlation function h(r)=g(r)-1. The last row at 2.0 °K is for distinguishable particles.

FIGURE CAPTIONS

Fig. 1 Energy and specific heat at SVP near T_λ. The solid lines are the experimental values. (The energy was taken from[5] and the specific heat from.[6]) The simulation results for the specific heat were obtained by differencing the energy values. The energy computed from ground state simulations[7] is denoted by the cross. The experimental value for T_λ (2.17 °K) is indicated by the arrow.

Fig. 2 (a) Radial distribution function for ^{4}He at 2 °K and SVP. The solid line is the neutron scattering result.[8] The circles are simulation results for bosons and the dashed line is for distinguishable particles.

(b) Single particle off-diagonal density matrix at 1.18 °K (top curve and open circles), 2.22 °K (middle curve and closed circles), and 3.33 °K (lower curve and open squares). Beyond 3 Å the vertical axis is enlarged by 10 times and the interpolating curves are omitted. The crosses denote the ground state results[12] which are indistinguishable from the T=1.18°K results for r<3 Å on this graph.

Fig. 3 (a) Percentage of atoms with zero momentum, $n_0(T)$, in ^{4}He at SVP. The indicated ground state value is from ref. 7.

(b) Momentum distribution from simulations at temperatures of 3.33 °K (——), 2.22 °K (---), 1.18 °K(o), and for distinguishable particles at 2.22 °K(●).

Fig. 1

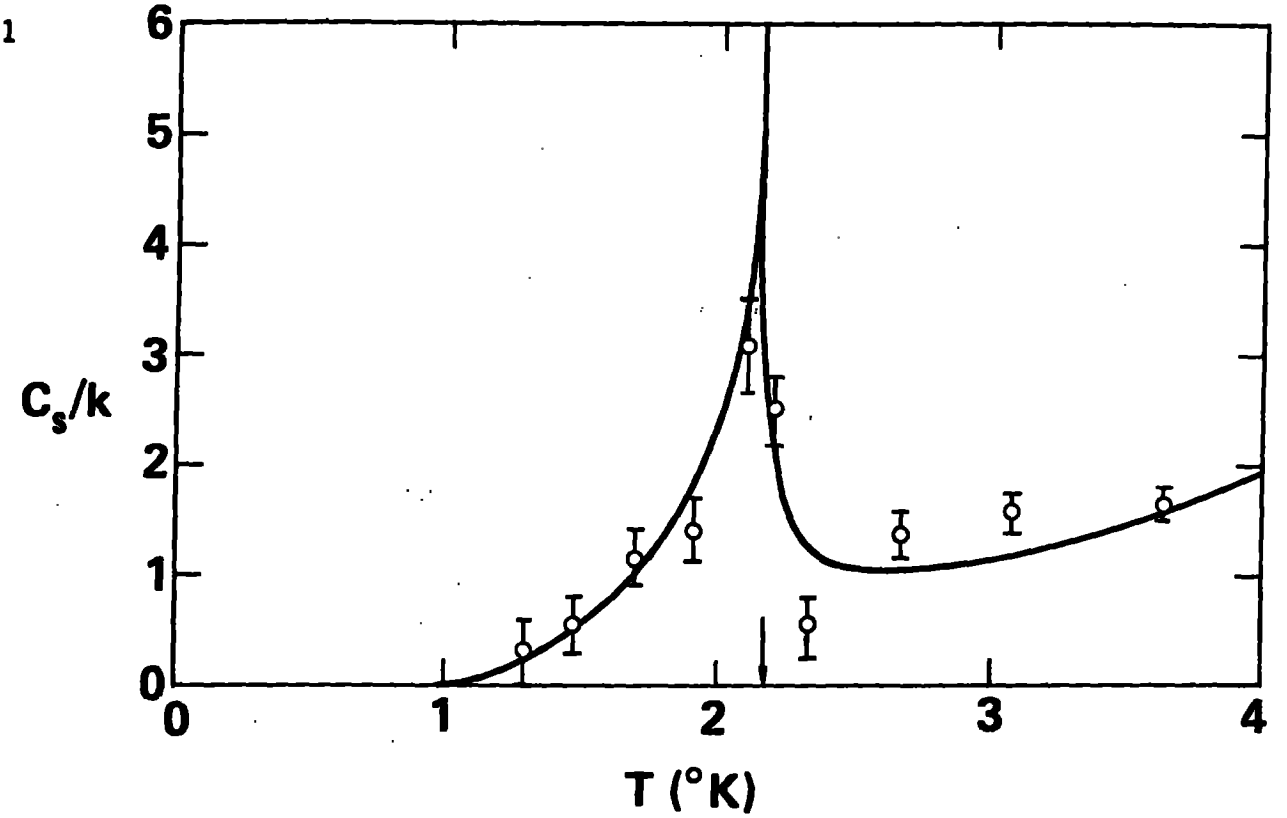

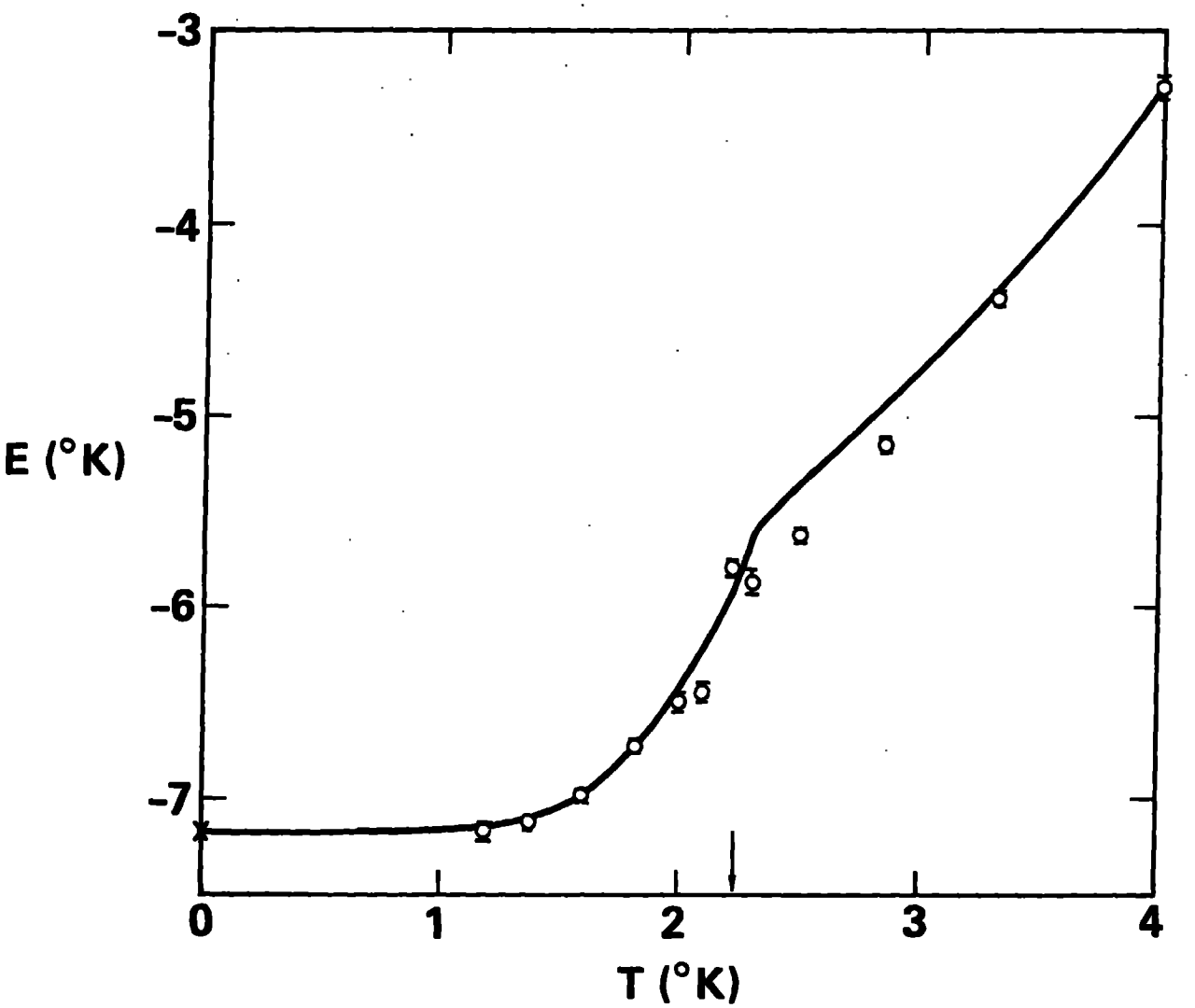

Fig. 2

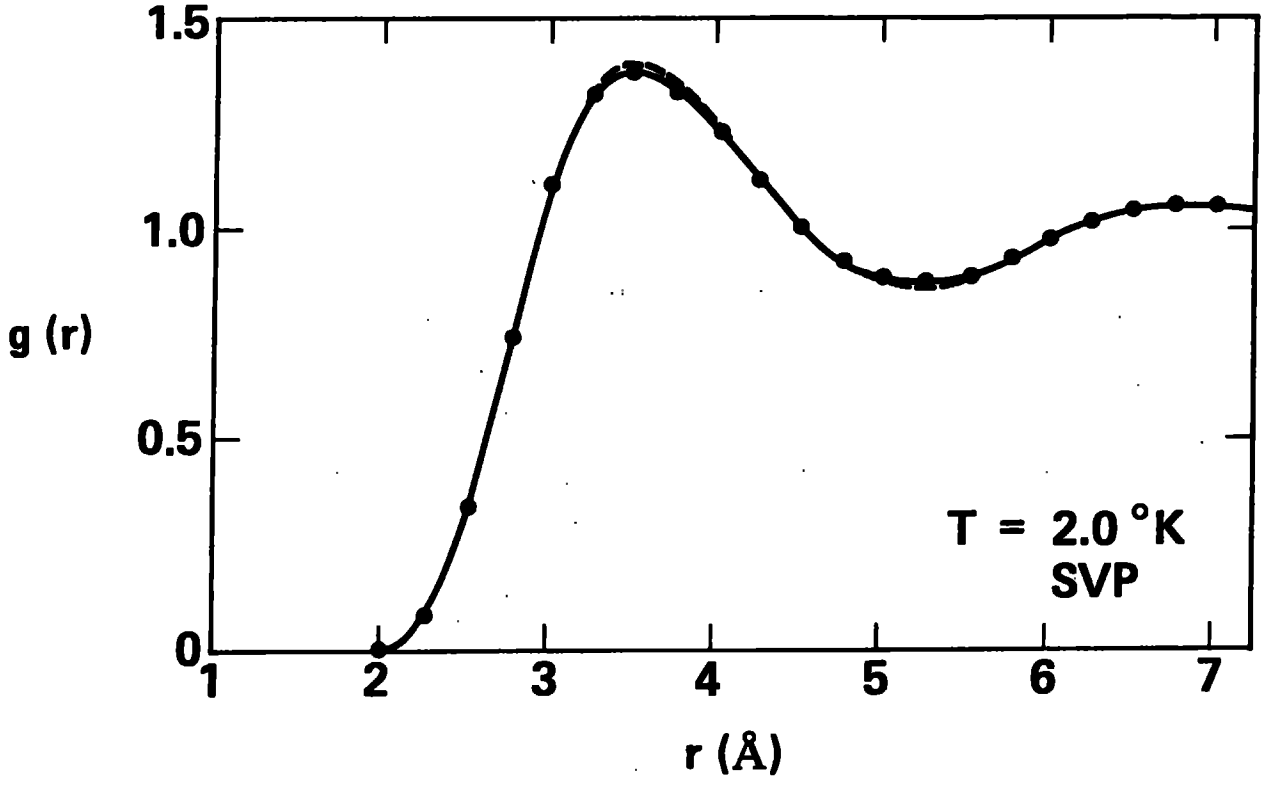
1.5
1.0
0.5
0
g (r)
T = 2.0 °K
SVP
1
2
3
4
5
6
7
r (Å)

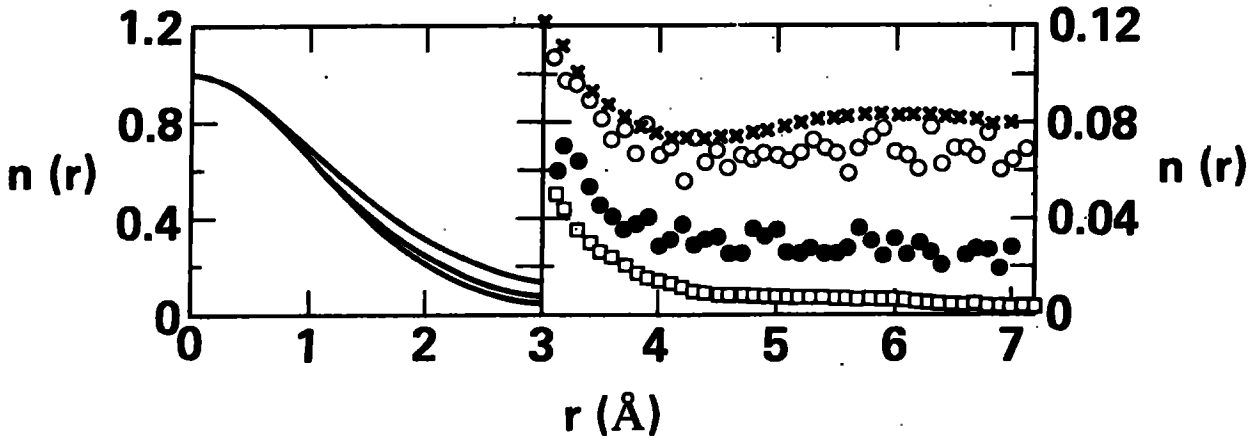
1.2
0.8
0.4
0
n (r)
0.12
0.08
0.04
0
n (r)
0
1
2
3
4
5
6
7
r (Å)

Fig. 3